IMMUNOTHERAPY



# Tracking the fate and origin of clinically relevant adoptively transferred CD8$^+$ T cells in vivo

Aude G. Chapuis,[1]* Cindy Desmarais,[2] Ryan Emerson,[2] Thomas M. Schmitt,[1] Kendall C. Shibuya,[1†] Ivy P. Lai,[1‡] Felecia Wagener,[1] Jeffrey Chou,[1§] Ilana M. Roberts,[1‖] David G. Coffey,[1] Edus H. Warren,[1] Harlan Robins,[1,2] Philip D. Greenberg,[1,3] Cassian Yee[1]*‡

**Adoptively transferred tumor-specific cells can mediate tumor regression in cancers refractory to conventional therapy. Autologous polyclonal tumor-specific cytotoxic T cells (CTLs) generated from peripheral blood and infused into patients with metastatic melanoma show enhanced persistence, compared with equivalent numbers of more extensively expanded monoclonal CTLs, and are associated with complete remissions (CRs) in select patients. We applied high-throughput T cell receptor Vβ sequencing (HTTCS) to identify individual clonotypes within CTL products, track them in vivo after infusion, and then deduce the preadoptive transfer (endogenous) frequencies of cells ultimately responsible for tumor regression. The summed in vivo posttransfer frequencies of the top 25 HTTCS-defined clonotypes originally detected in the infused CTL population were comparable with enumeration by binding of antigen peptide–human leukocyte antigen multimers, revealing that quantitative HTTCS is a reliable, multimer-independent alternative. The polyclonal CTL products were composed predominantly of clonotypes that were of very low frequency (VLF) in the endogenous samples, often below the limit of HTTCS detection (0.001%). In patients who achieved durable CRs, the composition of transferred CTLs was dominated (57 to 90%) by cells derived from a single VLF clonotype. Thus, HTTCS now reveals that tumor-specific CTLs enabling long-term tumor control originate from endogenous VLF populations that exhibit proliferative or survival advantages. Along with results indicating that naïve cell populations are most likely to contain cells that exist at VLF within the repertoire, our results provide a strong rationale for favoring T cells arising from VLF populations and with early differentiation phenotypes when selecting subset populations for adoptive transfer.**

## INTRODUCTION

Adoptive transfer of tumor-specific cytotoxic T cells (CTLs), a strategy demonstrating the capacity to eliminate cancer in an increasing number of settings, requires the in vivo establishment of a robust, persistent population of tumor-specific cells to prevent tumor recurrences (*1*, *2*). Our group has used the endogenous autologous T cell repertoire of patients as a readily accessible source of antigen-specific cells. In this approach, bulk peripheral blood mononuclear cells (PBMCs) are repetitively stimulated by dendritic cells pulsed with specific human leukocyte antigen (HLA)–restricted peptides from tumor antigens to increase the frequency of antigen-specific T cells. In our initial efforts, the responding cells were cloned by limiting dilution, one T cell clone was selected for expansion, and thus CTL infusion products represented progeny from one expanded cell (*3*–*8*). This strategy facilitated tracking by quantitative polymerase chain reaction (PCR)–based approaches, using primers flanking the clonal complementarity-determining region 3 (CDR3) (*5*, *7*). However, such monoclonal T cell products exhibited only a short survival in vivo (<14 days) in most of the patients, likely reflecting the extensive expansion required to attain therapeutic cell doses from a single reactive T cell in vitro and the associated terminal differentiation (*3*, *9*–*11*).

The availability of high-speed cell sorting based on peptide–major histocompatibility complex (pMHC) binding now enables infusion of CTLs that stem from a polyclonal tumor-specific repertoire (*12*). Additionally, in both murine and human studies, CD8$^+$ T cell culture conditions that include exposure to interleukin-21 (IL-21) during in vitro priming have been shown to facilitate greater expansion of the antigen-responding cells with less apoptosis (*13*–*17*). By using such strategies, therapeutic cell doses can be produced by ex vivo expansion in 4 to 6 weeks rather than 3 to 4 months, and the tumor-specific cells generated have a higher replicative capacity and less terminally differentiated phenotype in vivo (*8*, *12*, *18*). As a likely consequence of such technologies, infusion of polyclonal CTLs now produces enhanced in vivo persistence (>6 months) in a larger fraction of patients, which correlates with long-term tumor regression and improved disease control in a subset of patients (*19*, *20*).

Ample evidence suggests that the nature of the original parent T cell population is critical in determining the in vivo behavior of the expanded and infused CTLs (*10*, *17*, *21*–*23*). To elucidate the factors that might contribute to the persistence of these polyclonal, IL-21–primed CTLs that leads to clinical responses, we investigated the endogenous frequencies of the infused clonotypes that contribute to mediating and sustaining tumor regression. In the case of autologous adoptive transfers, expanded or infused polyclonal tumor-specific T cells necessarily originate from a patient's preexisting circulating T cell repertoire. After ex vivo stimulation and culture, the phenotype and frequency of the expanded CTLs are generally sufficiently altered such that the qualities of the parent cells cannot be determined from the characteristics of the cells at the time of infusion (*22*). However, the CTLs that persist express or acquire phenotypic and functional characteristics associated with long-lived memory T cells, including markers associated with survival (CD28, CD27, and CD127) (*24*, *25*) and lymph node homing (CD62L and CCR7) (*26*, *27*), and exhibit the capacity

[1]Program in Immunology, Fred Hutchinson Cancer Research Center, 1100 Fairview Avenue North, Seattle, WA 98109, USA. [2]Adaptive Biotechnologies, Suite 200, 1551 Eastlake Avenue North, Seattle, WA 98103, USA. [3]Department of Immunology, University of Washington, South Lake Union, Building E, 750 Republican Street, Seattle, WA 98109, USA.
*Corresponding author. Email: achapuis@fredhutch.org (A.G.C.); cyee@mdanderson.org (C.Y.)
†Present address: Western University of Health Sciences, 309 East 2nd Street, Pomona, CA 91766, USA.
‡Present address: MD Anderson Cancer Center, 7455 Fannin Street, Houston, TX 77054, USA.
§Present address: Pfizer Inc., 230 East Grand Avenue, South San Francisco, CA 94080, USA.
‖Present address: University of Washington, 1410 Northeast Campus Parkway, Seattle, WA 98195, USA.

for polyfunctional cytokine production [interferon-γ (IFN-γ), tumor necrosis factor–α, and IL-2] (*28*), suggesting that some of these characteristics are critical for persistence and tumor control (*20*).

We therefore used high-throughput T cell receptor Vβ sequencing (HTTCS) to sequence T cell receptor (TCR) Vβ regions in a massively parallel fashion and thereby assess clonotype evolution after infusions, determine the contribution of distinct cells, and investigate the original source of the cells whose progeny most likely made a major contribution to mediating tumor regression or control.HTTCS can discern individual TCR clonotypes in a polyclonal population with a limit of detection of 1 of 100,000 (0.001%) (*29*–*31*), and we first assessed whether this could enable in vivo tracking of the potentially thousands infused individual tumor-specific clonotypes. After demonstrating the accuracy of this approach, we then applied HTTCS to a set of 10 patients with metastatic melanoma who had detectable frequencies of transferred T cells after infusions. All patients had received polyclonal IL-21–primed T cell products expanded from unselected circulating T cell populations. We investigated the number of clonotypes that persisted after infusions, their individual frequencies, and the characteristics of the original source of the cells whose progeny most likely made a major contribution to mediating tumor regression or control.

## RESULTS

### Validation of HTTCS for tracking the frequency of transferred monoclonal CTLs in vivo

Among patients (Pt) who received monoclonal (M) T cells in a previous study (on "Protocol #2140" in Materials and Methods) (*7*), we analyzed the 2 (of 11 infused) in whom the transferred cells were detectable in vivo for >40 days after infusions (Table 1). Pt M2140-1 was infused with cells expanded from a melanoma-specific $CD8^+$ T cell clone: 99.4% of the cell infusion product bound the HLA A*0201–restricted melanoma-associated antigen recognized by T cells 1 (MART1) epitope$_{127–35}$ (AAGIGILTV) (A2/MART1) pMHC multimer (Fig. 1A). HTTCS revealed that one clonotype comprised 99.7% of all TCR reads; 29 other clonotypes detected with frequencies ≥0.001% (table S1) comprised the remaining 0.3% and were likely bystander or contaminant clonotypes derived from the irradiated allogeneic PBMCs used to expand the cells (Fig. 1B, upper pie plot). Pt M2140-2 was infused with $CD8^+$ T cells recognizing the HLA B*4402–restricted Tyrosinase$_{192–200}$ epitope (B44/Tyr), for which a pMHC multimer could not be synthesized. The cell product included a total of 868 clonotypes, of which the most prevalent single clonotype represented 94% of all TCR reads (Fig. 1B, lower pie plot). For both patients, the most prevalent HTTCS-detected clonotype was confirmed as the infused CTL clone by TCR Vβ quantitative PCR (table S2). We then compared the posttransfer in vivo frequencies of the most prevalent clonotype in each infusion product, as assessed by HTTCS, peptide-HLA multimer binding, and/or TCR Vβ quantitative PCR. For Pt M2140-1, frequencies obtained by HTTCS were 42.1, 0.84, and 0.61% of total TCR reads in PBMCs collected on days 4, 56, and 508 after transfer. By comparison, the frequencies by multimer staining were 40.0, 0.21, and 0.74%, and those by TCR Vβ–specific PCR were 48.5, 0.57, and 0.28% (Fig. 1C, upper graph). For Pt M2140-2, HTTCS frequencies were 21.5, 6.75, and 1.25% at days 4, 48, and 117 compared with 15.8, 3.0, and 0.71% using TCR Vβ–specific PCR (Fig. 1C, lower graph). Thus, for frequencies ≥0.001% of total T cells, HTTCS frequencies yielded results concordant to TCR Vβ–specific PCR and pMHC multimer binding, suggesting that HTTCS

**Table 1. Overview of protocol characteristics.** gp100, glycoprotein 100; NY-ESO1, New York esophageal antigen 1; MCPyV, Merkel cell polyoma virus; DC, dendritic cell; ND, not done; CY, cyclophosphamide.

| Protocol # | #2140 | #2225 | #2504 | #2558 |
|---|---|---|---|---|
| Disease type | Melanoma | Melanoma | Breast cancer | Merkel cell carcinoma |
| Target cell dose (cells/$m^2$) | $10^{10}$ | $10^{10}$ | $10^{10}$ | $10^{10}$ |
| CTL specificity | MART1/Tyrosinase/gp100 | MART1 | NY-ESO1 | MCPyV |
| Use of peptide-pulsed DCs | Yes | Yes | Yes | Yes |
| Use of IL-21 in cultures | No | Yes | Yes | Yes |
| Product clonality | Monoclonal | Polyclonal | Polyclonal | Polyclonal |
| Product median of CD27 expression (%) | 52.70 | 63.50 | ND | ND |
| Product median of CD28 expression (%) | 7.10 | 72.40 | ND | 6 |
| Product median of CD127 expression (%) | 0 | 36.20 | ND | 0 |
| Product median of CD62L expression (%) | 0 | 0 | ND | ND |
| Product median of CCR7 expression (%) | 0 | 0 | ND | ND |
| Preinfusion conditioning | CY (4000 mg/$m^2$) over 2 days | CY (300 mg/$m^2$) | CY (2000 mg/$m^2$) | None |
| Number of patients infused | 11 | 10 | 1 | 1 |
| Persistence >40 days, *n* (%)* | 2/11 (18) | 10/10 (100) | 1/1 | 1/1 |

*% Multimer$^+$ $CD8^+$ cells, ≥0.1%.

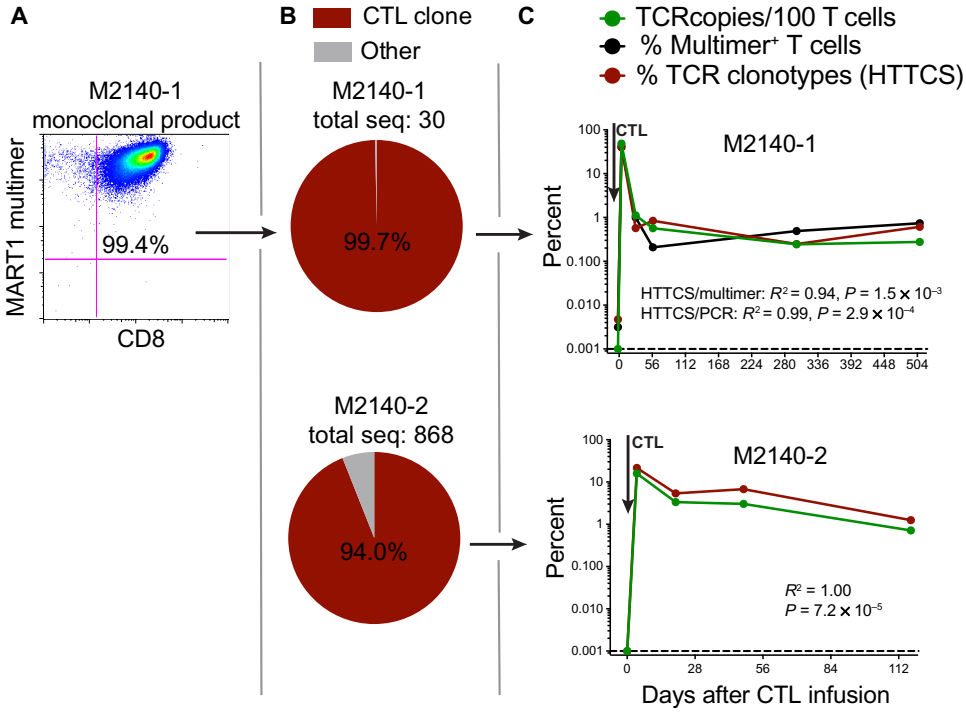


**Fig. 1. Characteristics of monoclonal CTL products and concurrence of clonotype frequencies determined by TCR Vβ PCR, multimer stains, and HTTCS in vivo.** (**A**) Scatter plot showing binding of the monoclonal cells to CD8 (*x* axis) and HLA A*0201–restricted MART1$_{27–35}$ (*y* axis). (**B**) Pie plots showing the percent of individual clonotypes composing the monoclonal CTL products. The frequency of the specific clone is overlaid on the plots. The total number of sequences detected in the products is stated above each plot. (**C**) Pre- and postinfusion TCR Vβ copies per 100 CD8 T cells (solid green circles), % multimer$^+$ T cells (solid black circles), and % clonotypes in PBMCs (solid red circles) for two patients who received monoclonal CTL products. Vertical arrows indicate CTL infusions. Dashed red lines represent the limit of detection of frequencies by HTTCS. Significance values of the correlation ($R^2$ and *P* values) between HTTCS/multimer and HTTCS/TCR copies per 100 cells are depicted below each graph.

can be used to quantitatively track the frequency of infused monoclonal CD8$^+$ T cells in vivo.

## HTTCS accurately tracks the in vivo frequencies of adoptively transferred polyclonal CTLs

We next analyzed PBMCs from 10 patients who had each received one infusion of $10^{10}/m^2$ polyclonal (P) CTLs specific for A2/MART1 on a previous study (on "Protocol #2225" in Materials and Methods and Table 1) (*20*). HTTCS detected between 56 and 2036 (mean, 555.4) clonotypes in the polyclonal infusion products from Pt P2225-1 to Pt P2225-10 (Fig. 2A). The most prevalent clonotype comprised between 4 and 77% of the total cells in each infusion (mean, 33.3%), and the 25 most prevalent clonotypes together comprised between 35.0 and 99.9% (mean, 78.4%) of the total cell products. This HTTCS analysis was performed on infusion products selected for binding pMHC multimers with >99% purity. The limit of pMHC detection is typically ≥0.01% of CD8$^+$ T cells, which is at least 10-fold less sensitive than HTTCS. Thus, HTTCS of infusion products that have been selected by pMHC multimer binding is likely to also include contaminant clonotypes. To avoid tracking these bystander clonotypes after adoptive transfer, we excluded from analysis those clonotypes that had higher frequencies in preinfusion PBMCs compared with their frequencies within the CTL products, because these clonotypes likely reflected nonexpanded bystander cells that decreased in frequency through the cell culture process (table S3). A total of 86 clonotypes (average, 0.014% of total CTL products) with frequencies of 0.001 to 8.85% (mean, 0.35%) were thus identified and removed from our analysis. Tracking the sum of the frequency of all expanded and infused clonotypes by HTTCS yielded near-concurrent results with those obtained by tracking pMHC multimer binding for all patients who received polyclonal products (Fig. 2B). Thus, HTTCS appears to accurately track the in vivo frequencies of infused polyclonal CTLs.

## In vivo specific clonotype frequencies increase as a consequence of adoptive transfer

To affirm that the postinfusion increase in clonotype frequencies is a reproducible consequence of the CTL infusions, we assessed the frequency of individual infused clonotypes for two patients who each received two polyclonal infusions, 30 or 37 days apart ("Protocol #2504" and "Protocol #2558" in Materials and Methods and Table 1) (*32*). Although the clonotypes constituting the largest fraction of the patients' first and second infusates were shared, clonotype frequencies did vary as a likely consequence of the culture process, which uses an aliquot of the first CTL culture or infusion to expand sufficient cells for a second infusion (Fig. 3A). The sum of all shared clonotypes was tracked in PBMCs before and after each infusion (Fig. 3B), as was the individual contribution of the top 25 and all 10 clonotypes for Pt P2504-1 and Pt P2558-1, respectively (Fig. 3C). Before infusions, all clonotypes were detected in PBMCs with frequencies of <0.01% (maximum, 0.0097; median, 0.001%) and 0.09% (maximum, 0.085%; median, 0.0028%) for Pt P2504-1 and Pt P2558-1, respectively. The frequency of the clonotypes peaked between days 1 and 7 after the first infusion (Pt P2504-1: maximum TCR sequence 2, 1.5%; median for first 25 clonotypes, 0.06%; Pt P2558-1: maximum TCR sequence 5, 2.73%; median for all 10 clonotypes, 0.35%), and the frequencies decreased over 14 or 30 days to near or at baseline levels. The same clonotypes then peaked again 1 to 7 days after the second infusion, albeit at lower frequencies (Pt P2504-1: maximum TCR sequence 11, 0.64%; median, 0.05%; Pt P2558-1: maximum TCR sequence 1, 0.68%; median, 0.15%). Thus, the postinfusion changes in clonotype frequency appear to be a consequence of the infusion of antigen-specific CTLs and not coincidental variations within the endogenous TCR repertoire. Notably, for these two patients, no correlation could be established between the frequency of the clonotypes in the infused product and the peak frequencies after infusion.

## Single, immunodominant persistent clonotypes are associated with CRs after adoptive transfer

Of the 10 patients with metastatic melanoma who received A2/MART1-specific polyclonal CTLs, 2 achieved complete remission (CRs), as evaluated by the immune-related response criteria (IrRC)

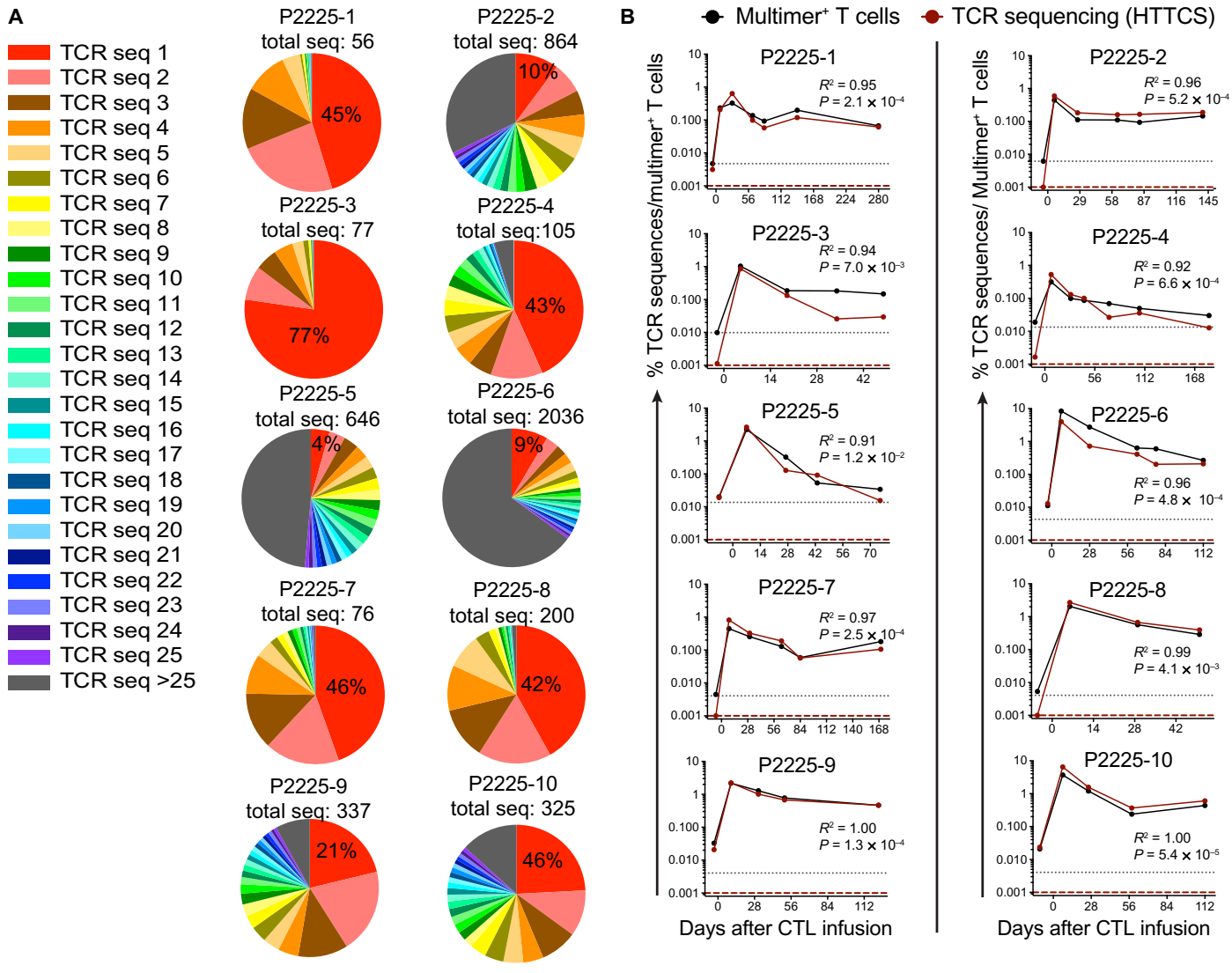


**Fig. 2. Characteristics of polyclonal products and concurrence of clonotype frequencies determined by HTTCS and multimer staining.** (**A**) Pie plots show the frequency of the first 25 TCR clonotypes in polyclonal products (shaded in color) and the remainder of the clones (shaded in gray). The total number of clonotypes in the products is indicated above each plot. The frequency of the most prevalent clonotype (in red) is indicated. (**B**) Percent antigen-specific clonotypes obtained by HTTCS (solid red circles) and % multimer$^+$ T cells (solid black circles) before (left-most time point) and after infusions (infused on day 0) for 10 patients who received polyclonal antigen-specific products. Vertical arrows indicate CTL infusions. Dashed red lines represent the limit of detection for HTTCS, and dotted gray lines represent the limit of detection for multimer staining, which is dependent on the ratio of CD8$^+$ to CD4$^+$ T cells and varies for each patient. Significance values of the correlation ($R^2$ and $P$ values) between HTTCS and multimer are depicted on the right side of each graph.

(*33*), 2 had partial remissions (PRs), 3 had stable diseases (SDs), and 3 had progressive diseases (PDs) as best response (table S4) (*19*, *20*). The frequencies of the first 25 most prevalent clonotypes detected in each cell product were individually tracked in vivo after adoptive transfer (Fig. 4A, colored lines), as were the sum of the remaining clonotypes (Fig. 4A, gray lines). In the two patients who achieved CRs after infusion (Pt P2225-1 and Pt P2225-7), only one individual clonotype remained detectable at sustained frequencies higher than those of other infused clonotypes (0.056% at day 280 and 0.093% at day 175 after infusion for Pt P2225-1 and Pt P2225-7, respectively) and represented most (>99%) of the detected antigen-specific cells after infusion (Fig. 4A, red arrows). Clonotype half-lives ($t_{1/2}$) (see "Statistical analysis") were determined for each patient and grouped according to best clinical response (Fig. 4B). For patients who achieved CRs (Pt P2225-1 and Pt P2225-7), the immunodominant clonotypes (Fig. 4B, red arrows) had $t_{1/2}$ of 173 and 132 days, which was about seven and five times longer, respectively, than the median $t_{1/2}$ of all infused clonotypes for Pt P2225-1 to Pt P2225-10 (24.8 days). Along with the higher expression of Ki67 by the transferred pMHC multimer–binding cells—composed by most of the dominant clonotypes—compared with multimer$^-$ cells (table S5) (*7*, *20*), these findings indicate that the immunodominant CTLs had the capacity to expand and persist. For the remaining patients, the average $t_{1/2}$ of clonotypes after transfer was 53 and 31 days for patients who achieved a PR as best response (Pt P2225-9 and Pt P2225-10); 44, 46, and 21 days for patients who achieved an SD (Pt P2225-2, Pt P2225-4, and Pt P2225-6);

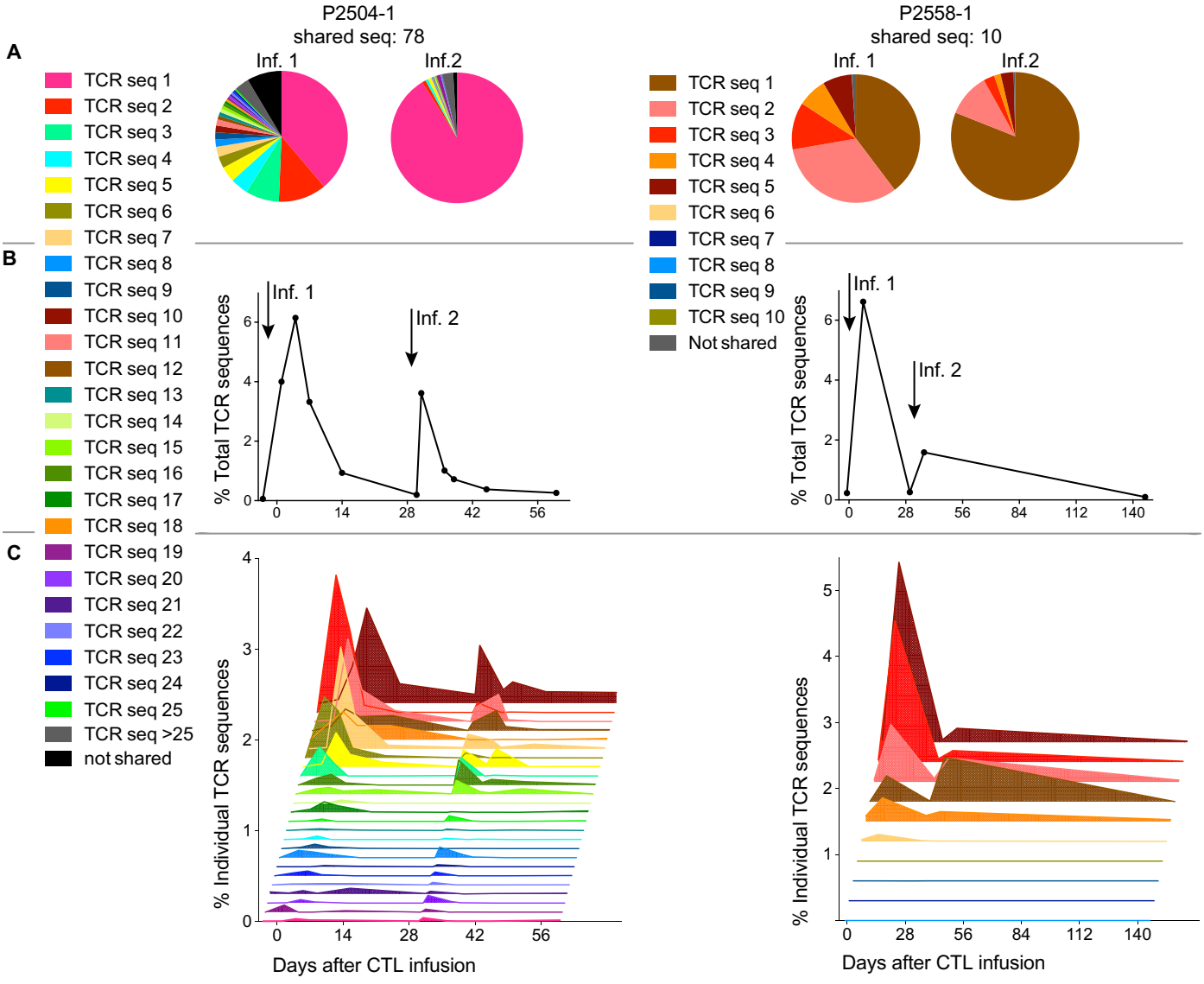


**Fig. 3. Reproducibility of peak clonotype frequencies in vivo after infusions.** (**A**) Pie plots showing the most prevalent 25 clonotypes shared for infusions 1 (Inf. 1) and 2 (Inf. 2) for Pt P2504-1 (left) and the most prevalent 10 clonotypes for Pt P2558-1 (right, shaded in color), as well as the remaining, not shared clonotypes present in the infusion products (shaded in gray). TCR sequences that were not shared between the two products are shaded in black. The number of shared sequences is indicated above the pie plots. (**B**) The sum of the percents of antigen-specific clonotypes (left *y* axis) in PBMCs before and after infusions is shown for Pt P2504-1 (left) and Pt P2558-1 (right). (**C**) The individual percent contribution of the most prevalent 25 shared antigen-specific clonotypes (left *y* axis) is shown for Pt P11 (left) and Pt P12 (right).

and 13, 15, and 14 days for patients who progressed (Pt P2225-3, Pt P2225-5, and Pt P2225-8). When all clonotype $t_{1/2}$'s were grouped according to patients' best response (Fig. 4C), the $t_{1/2}$ differences were statistically significant between patients who obtained CRs, PRs, SDs, and PDs. Thus, prolonged in vivo persistence of transferred clonotypes is associated with, and presumably important for, tumor control by transferred CTLs.

## Preexisting clonotype frequencies provide insights into the nature of persisting CTLs

The number of clonotypes comprising the polyclonal cell products for Pt P2225-1 to Pt P2225-10 was between 56 and 2036, with a median of 262.5 clonal sequences (table S2). However, most clonotypes present in cell products (range, 43 to 1275; median, 160) were detected by HTTCS, with frequencies below 0.001% (the limit of detection), in PBMCs obtained before and after infusion and constituted only a minor fraction of the total infusion product (range, 0.82 to 24.7%; median, 2.26%) (Fig. 5A, gray areas). As stated before, a clonotype with a frequency in the CTL product that was less than its corresponding frequency in the preinfusion PBMCs was defined as having not expanded during the culture process (table S2, bottom row). These clones comprised a minor fraction of the final infusion product, with a median of 0.02% (range, 0 to 0.61%) (Fig. 5A, purple areas), and were not further monitored. We found that clonotypes detected in any postinfusion PBMC sample, but not detected in preinfusion samples (range, 10 to 205; median, 56 sequences), were the dominant components of the final cell product (range, 74.68 to 98.97%; median, 97.67%) (Fig. 5A, blue areas), implying preferential expansion from individual

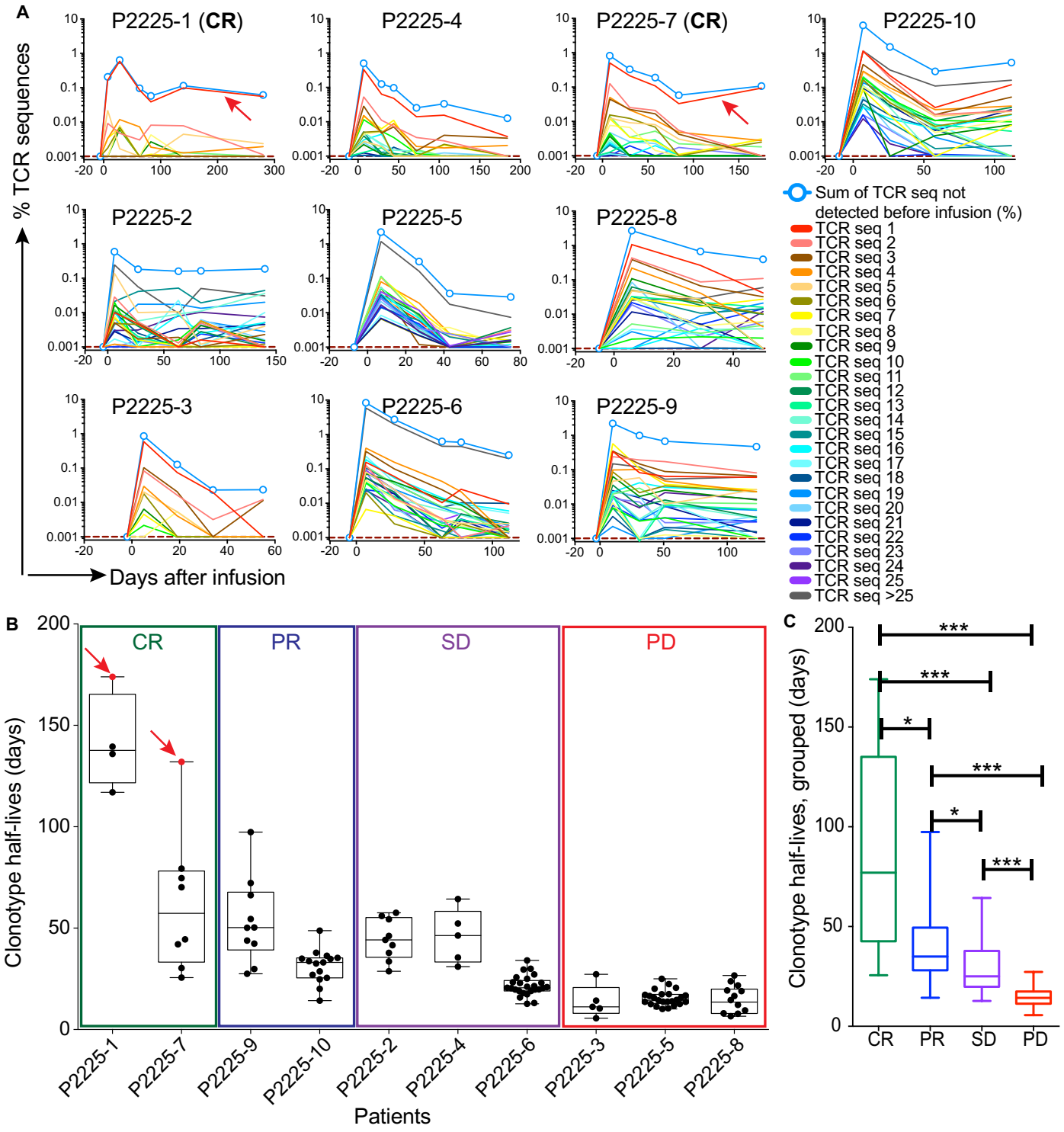


**Fig. 4. Composition of infused products and persistence or frequency of TCR subsets in vivo.** (**A**) Percent clonotypes detected at any time point after infusions (open blue circles). The individual percent contribution of the most prevalent 25 antigen-specific clonotypes in the infused products (left *y* axis) is shown (colored lines), as well as the sum of the remaining sequences in the products (gray lines), before (left-most time point) and at selected time points after infusions (day 0). Red arrows indicate the immunodominant clonotypes for Pt P2225-1 and Pt P2225-7, who achieved a CR (indicated) as best response. (**B**) Half-lives of clonotypes for each patient grouped according to their best response. Green box, CRs; blue box, PR; purple box, SD; red box, PD. Arrows pointing to red circles indicate the immunodominant clonotypes for Pt P2225-1 and Pt P2225-7. (**C**) Box-and-whisker plots of the $t_{1/2}$ grouped according to patients' best responses. $^{*}P \leq 0.05$, $^{***}P \leq 0.0005$.

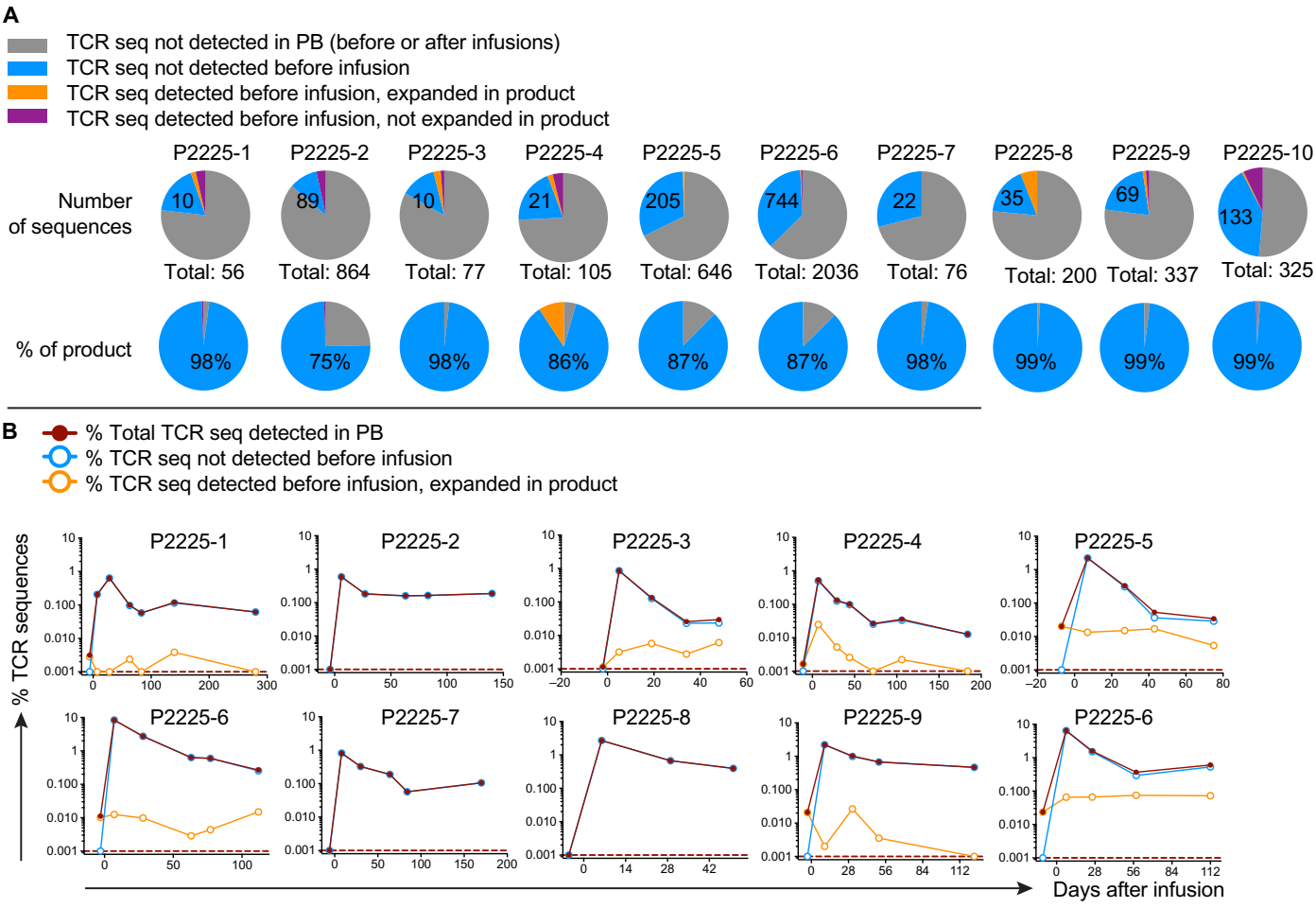


**Fig. 5. Persistence or frequency of different clonotype subsets in vivo.** (**A**) Pie plots showing the number (top row) and percentage (bottom row) of clonotypes composing the infused polyclonal products. Clonotypes in the infusion products that were below the limit of detection either before or at any time point after infusions (gray area). Clonotypes detected at any time point after infusions that were not detected in PBMCs (PB) before infusions (blue area). The numbers of clonotypes composing the blue area for each patient are shown on the top row, and their respective percentages are shown on the bottom row. Orange, sum of the clonotypes detected in PBMCs before infusions, expanded in the infusion product; purple, sum of clonotypes detected in PBMCs before infusions, not expanded in the infusion product. (**B**) Percent total antigen-specific TCR sequences (solid red circles); percent total TCR sequences detected at any time point after infusions that were not detected in PBMCs before infusions (open blue circles); percent total TCR sequences detected in PBMCs before infusions, expanded in the infusion product (open orange circles), before and at selected time points after infusions.

parental clonotypes with frequencies <0.001%, that is, a very low frequency (VLF) population. The immunodominant clonotypes in both patients who achieved CRs (Pt P2225-1 and Pt P2225-7) (Fig. 4, A and B, red arrows) were derived from their respective VLF populations. Clonotypes expanded in the cell infusion product that were detectable in PBMCs before infusion were less prevalent (range, 0 to 6; median, 2 sequences), comprising <10% (range, 0 to 9.22%; median, 0.03%) of the final cell products that were infused (Fig. 5A, orange areas). The frequencies of all expanded clonotypes were summed at multiple time points after infusion (Fig. 5B, solid red circles) and further subdivided into previously undetected clonotypes (Fig. 5B, open blue circles) versus previously detected clonotypes (Fig. 5B, orange open circles). Previously undetected clonotypes represented most of the cells in both infusion products and the detected clonotypes in posttransfer PBMCs, whereas previously detected clonotypes comprised a small fraction of infused products and a minority of posttransfer clonotypes.

To assess the likelihood that the preferentially expanded and infused clonotypes originated from a distinct parental T cell subpopulation, we assessed the propensity for clonotypes present in the three sets of normal donor PBMCs to exhibit a mostly antigen-experienced or naïve phenotype. Overall, clonotypes with frequencies <0.001% in PBMCs were 15 times more likely (72 ± 2% versus 5 ± 3%) to have originated from a $CD3^+CD45RA^+$ [primarily naïve T cells ($T_N$)] VLF population than from a $CD3^+CD45RO^+$ (mostly antigen-experienced cells) population (fig. S1).

## DISCUSSION

The use of HTTCS to examine TCR clonotypes of defined antigen specificity before infusion, through in vitro culture and after adoptive transfer, has provided a means to monitor the accumulation and in vivo persistence of individual clonotypes within a polyclonal population. This technology provides concordant results with frequency

analyses by quantitative PCR of defined TCRs, which has more limited utility but can be used for tracking monoclonal cell products, and by pMHC multimer stains, which can be used to track polyclonal and monoclonal products but does not distinguish individual clonotypes (*5*, *7*, *20*, *34*, *35*). HTTCS essentially provides a "natural barcode sequence" through the specific CDR3 TCR sequences of all clonotypes in an infused CTL cell product, enabling the identification of the cell or clonotype of origin within preinfusion donor PBMCs, measuring the expansion of each individual clonotype in the infusion product, and monitoring their individual in vivo fates after infusions (*29*–*31*). These results can be correlated with clinical outcomes, which should facilitate the development of methods to preferentially isolate or generate cells that will have greater therapeutic efficacy.

We were surprised to observe that the vast majority of CTLs expanded in the infusion product originated from rare T cells. To increase the probability of generating autologous antigen-specific cells for adoptive transfer, the culture methods used in this study were aimed at expanding as many T cells as possible, without regard for a specific substrate T cell subset (*20*). Thus, autologous MART1-specific T cells "competed" with each other in the culture system, and certain clonotypes with preinfusion frequencies <0.001% demonstrated an increased fitness and preferentially expanded. These were also the cells that comprised most of the antigen-specific cells that were detectable and persisted after infusion. Thus, the culture system fostered the expansion of fit cells that, despite having the capacity to recognize the tumor antigen, had a lower likelihood of already having been expanded in vivo in the tumor-bearing patient. By contrast, tumor-specific clonotypes that were more abundant in preinfusion PBMCs, with frequencies >0.001%, were generally less numerous in the final cell products and persisted less robustly in vivo after infusion, suggesting that these cells both expanded less well ex vivo and were less fit for survival after infusion. This latter observation is consistent with the poor expansion of tumor-specific cells that have been driven to exhaustion by a persistent antigenic burden (*36*).

It is known that the qualities of the parent T cell from which tumor-specific CTLs originate before ex vivo expansion play a critical role in in vivo persistence, survival, and proliferation after transfer (*1*, *2*). $CD8^+$ T cells can be separated into distinct subsets based on phenotypic markers that distinguish cells with different molecular programs and biologic functions. These CD8 subsets include $T_N$ and antigen-experienced cells, with the latter further subdivided into at least memory stem cells ($T_{SCM}$), central memory cells ($T_{CM}$), effector memory cells ($T_{EM}$), and terminal effector cells ($T_{eff}$) (*10*, *14*, *17*, *21*, *22*, *37*, *38*). In prevention models, $T_{CM}$ are generally superior to $T_{EM}$, presumably reflecting the distinct ability of $T_{CM}$ to form long-lasting memory, rapidly proliferate and expand after reencountering antigen, and produce abundant differentiated $T_{EM}$ (*10*, *21*, *22*). By contrast, in therapy models of established tumors and of chronic infection, transferred cells derived from $T_N$ are generally superior to $T_{CM}$, with an enhanced ability to provide sustained proliferation and in vivo expansion, leading to enhanced persistence and antitumor activity. This likely reflects both the greater replicative potential of $T_N$-derived cells and the fact that $T_{CM}$ may already be programmed to undergo apoptosis or become functionally exhausted if stimulation persists and the antigen is not rapidly cleared (*17*, *23*). Within the $T_N$ compartment ($CD45RA^+62L^+$), the small subset of $T_{SCM}$, distinguished by CD95 expression, appeared to retain the plasticity of $T_N$ and the self-renewal capacities of $T_{CM}$ (*38*), functioned better than $T_{CM}$ in tumor therapy models, and persisted for years after transfer into humans (*39*–*41*).

Although available clinical reagents could not distinguish the origin of cells at the time of infusion because expanded CTLs derived from $T_N$, $T_{CM}$, or $T_{EM}$ mostly display a differentiated $T_{EM}$ phenotype after in vitro expansion (*8*, *20*, *22*), our data set does provide insights into the likely origin(s) of the most effective cells. All cells obtained from the patients were stimulated with antigen-pulsed dendritic cells in the presence of IL-21 that facilitates the expansion of antigen-specific CTLs with low initial endogenous frequencies (*15*). The effects of IL-21 exposure during priming of antigen-specific $CD8^+$ $T_N$ have been best characterized and shown to help imprint a central memory program after antigen-specific stimulation, with limited differentiation of the expanded cells promoting survival, expansion, and in vivo persistence after infusion in murine models and human trials (*8*, *14*, *42*, *43*). However, the effect of IL-21 on previously exposed antigen-experienced memory cells during stimulation is less clear (*43*, *44*). Our analysis of normal donors suggests that clonotypes with PBMC frequencies <0.001% were 15 times more likely to be included in a $CD45RA^+$ subset, which includes mostly $T_N$ but also $T_{SCM}$, compared with $CD45RA^-$ subsets that include $T_{eff}$, $T_{EM}$, and $T_{CM}$. These findings are consistent with murine studies, where antigen-specific naïve precursor frequencies were estimated at ≤1 of 200,000 cells (*45*) and where most of the naïve CD8 T cell TCRβ sequences were found at a very low clonotype frequency (*46*). Together, these data support the notion that antigen-naïve T cells are included in VLF populations. Although speculative, cells derived from VLF populations in our study might have been more likely to originate from a naïve rather than antigen-experienced subset. However, this could not be ascertained because of the logistical impossibility of sampling all preinfusion cells to obtain their phenotypes (*7*, *20*). It is plausible that some $T_{CM}$ and $T_{SCM}$ may also be found among the VLF populations, because these early differentiation phenotypes may have experienced limited in vivo expansion (*38*). However, regardless of origin, parent cells whose progenies have the potential to ultimately persist, either assisted by IL-21 exposure or due to their intrinsic nature, are rare in the repertoire. By contrast, in vivo expanded cells with higher intrinsic frequencies are apparently not suitable substrates for achieving sustained responses by T cell infusion.

Our findings also show that within VLF populations, only a minority of CTLs are poised to produce offspring that can mediate sustained clinical responses. In this series of patients with metastatic melanoma, HTTCS tracking of infused clonotypes showed that the antigen-specific response in PBMCs of patients who reached CRs was largely dominated by a single immunodominant CTL clone, derived from a VLF population, which remained detectable at high frequencies over time. Although no pre- or posttumor biopsies were obtained from these patients to assess the presence of these clonotypes at the tumor site, the development of vitiligo in Pt P2225-1 (*19*) suggests an ongoing MART1-specific on-target, off-tumor effect. Along with the capacity of the immunodominant CTLs for sustained proliferation, reflected by their Ki67 expression and markedly prolonged $t_{1/2}$ (>100 days) in PBMCs compared with other simultaneously transferred clonotypes, these CTLs were likely instrumental for tumor elimination either through a direct anti-MART1 effect or by facilitating the development of secondary responses (*19*, *20*). For these two patients, only 1 of 56 (1.8%) and 1 of 76 (1.3%) infused clonotypes persisted and mediated or contributed to antitumor responses. These results are reminiscent of the proliferation and expansion of a very limited number of T cell clones at the tumor site in patients who presented clinical responses to immunomodulatory agents (*47*).

The application of HTTCS to this clinical trial has provided unique insights by enabling tracking of individual clonotypes. Whether the properties of the parental cells from which the clonotypes were derived, and/or the affinity of the specific TCRs, conferred superior efficacy in the patients who experienced CRs remains unclear. Because long-term T cell survival can be enhanced by antigenic exposure, cells that carry high-affinity TCRs that can signal in the context of low levels of antigen presentation (*2*, *48*, *49*), as is the case for most "self" tumor antigens (*50*), are likely to have a postinfusion survival advantage compared with those that carry low-affinity TCRs (*51*). Of the 10 patients we studied, only 2 of 4722 MART1-specific infused clonotypes (0.04%) demonstrated an immunodominant antitumor effect. Thus, a better understanding of such TCRs, and the intrinsic cellular properties associated with this rare feature, could direct strategies to endow cell therapy products with enhanced antitumor efficacy. Such TCRs can be identified by HTTCS and are paramount candidates for isolation use in adoptive T cell therapies, in which TCR genes are transduced into optimal T cell subsets for patients with appropriately matched HLA types. This strategy might be used to broadly confer antitumor efficacy to a wider range of patients with metastatic diseases.

## MATERIALS AND METHODS

### Clinical protocols and patient characteristics

All clinical investigations were conducted according to the Declaration of Helsinki principles. All clinical protocols were approved by the Fred Hutchinson Cancer Research Center (FHCRC) Institutional Review Board and the U.S. Food and Drug Administration. All patients provided written informed consent.

### Treatment plans (Table1)

***Protocol #2140.***

Pt M2140-1 and Pt M2140-2 with metastatic melanoma received cyclophosphamide (4000 mg/m$^2$) administered over 2 days before the infusion of $10^{10}$ monoclonal melanoma-specific CTLs/m$^2$, followed by low-dose subcutaneous IL-2 (250,000 U/m$^2$) twice daily for 14 days (NCT 00438984) (*7*). Pt M1 and Pt M2 received CTLs specific for A2/MART1 and HLA B*4403–restricted Tyrosinase$_{192–200}$ (SEIWRDIDF), respectively. We specifically analyzed the 2 of 11 patients who received monoclonal products and demonstrated postinfusion in vivo persistence for a direct assessment of the equivalence of multimer staining, CDR3 PCR, and HTTCS on a unique CTL clone.

***Protocol #2225.***

Pt P2225-1 to Pt P2225-10 with metastatic melanoma received cyclophosphamide (300 mg/m$^2$) before the infusion of $10^{10}$ polyclonal A*0201–restricted MART1$_{27–35}$ CTLs/m$^2$, immediately followed by low-dose subcutaneous IL-2 and ipilimumab (3 mg/kg; anti–CTL-associated protein 4, YERVOY; Bristol Myers Squibb) (*52*) every 3 weeks for a total of four doses (NCT 00871481) (*20*). Radiologic responses were evaluated after infusion according to the IrRC (fig. S1) (*33*). Compared with monoclonal products, a higher fraction of polyclonal products expressed the markers CD27, CD28, and CD127 associated with memory. Whereas 100% (10 of 10) of polyclonal products persisted, only 18% (2 of 11) of monoclonal products persisted beyond 40 days in vivo (Table 1).

***Protocol #2504.***

Protocol #2504 is a single-patient protocol for Pt P2504-1 with metastatic breast cancer whose tumor expressed NY-ESO1. The patient received cyclophosphamide (2000 mg/m$^2$) administered 3 days before infusion of $10^{10}$ polyclonal HLA A*0201–restricted NY-ESO1$_{157–165}$ (SLLMWITQC) CTLs/m$^2$. Thirty days later, the patient received the same cell dose preceded by cyclophosphamide (300 mg/m$^2$).

***Protocol #2558.***

Protocol #2558 is a single-patient protocol for Pt P2558-1 with metastatic Merkel cell carcinoma whose tumor expressed the MCPyV (*32*). The patient received $10^{10}$ polyclonal HLA A*2402–restricted MCPyV LT-Ag$_{92–101}$ (EWWRSGGFSF) preceded by intralesional IFN-β1B ($3 \times 10^6$ IU) to a pancreatic metastasis and followed by low-dose subcutaneous IL-2. Thirty-one days later, the patient received the same cell dose, this time preceded by a single 8-Gy fraction of radiation to a remaining metastasis, followed by 14 days of low-dose subcutaneous IL-2.

### Generation and expansion of monoclonal tumor-specific CTL products (without IL-21)

For protocol #2140, which involved monoclonal tumor-specific cells, cell processing was as previously described (*7*). Briefly, PBMCs were collected by leukapheresis, and all ensuing ex vivo manipulations were performed in the clinical Good Manufacturing Practices Cell Processing Facility of the FHCRC (*12*). Donor PBMCs were stimulated three times for 7- to 10-day cycles, with autologous DCs pulsed with the A2/MART1 peptide (AnaSpec) at a DC-to-effector ratio of 1:2 to 10 to obtain sufficient frequencies (>5%) of MART1-reactive CD8$^+$ T cells. On day 2 of each stimulation, the $\gamma_c$-chain cytokines IL-2 (12.5 IU/ml), IL-7 (5 ng/ml), and IL-15 (1 ng/ml) were added. Cultures that contained ≥5% specific CD8$^+$ T cells, assessed by multimer analysis, were cloned by limiting dilution and then stimulated twice using the rapid expansion protocol (*4*). CTL products were frozen, thawed, and washed before infusion for a total production time of 12 to 13 weeks.

### Generation and expansion of polyclonal tumor-specific CTL products (with IL-21)

For protocols #2225, #2504, and #2586, polyclonal tumor-specific cell products were generated as previously described (*12*, *20*). Briefly, PBMCs were depleted of CD25$^+$ T cells (Miltenyi Biotec Inc.) to eliminate regulatory T cells and were stimulated for 7 days twice with autologous DCs pulsed with MART1$_{26–35}$. DC stimulations were supplemented with the same $\gamma_c$-chain cytokines plus IL-21 (30 ng/ml) on day 1. Cultures that contained ≥5% specific CD8$^+$ T cells were clinical grade–sorted (BD Influx Cell Sorter, BD Biosciences) and stimulated twice using the rapid expansion protocol. The total production time was 6 weeks.

### CTL tracking by pMHC multimers

The sensitivity of multimer staining was fixed at 0.1% of total CD8$^+$ T cells for monoclonal products (*7*) and at 0.05% for polyclonal products, as previously described (*20*). To compare the multimer stain tracking results expressed as a percentage of CD8$^+$ T cells with HTTCS expressed as a percentage of CD4$^+$ and CD8$^+$ T cells, multimer results are reported as a percent of CD4$^+$ and CD8$^+$ cells using the following formula: (% multimer$^+$ CD8$^+$ T cells) × ([% total CD8$^+$ T cells in each sample]/([% total CD8$^+$ T cells] + [% total CD4$^+$ T cells])).

### CTL tracking by quantitative PCR

Primers flanking the CDR3 region of infused melanoma-specific CTL clones were designed, as previously described (*5*, *7*). Total CD4$^+$ and CD8$^+$ T cells were determined by flow cytometry, and the

following formula was used to determine TCR copies per 100 T cells: 100/([% total $CD8^+$ T cells in each sample] + [% total $CD4^+$ T cells in each sample]*[TCR copies/{β-actin copies/2}*100]).

### DNA extraction and immunosequencing

DNA was extracted from CTL products and whole PBMCs using Qiagen Maxi DNA isolation kits (Qiagen Inc.). TCRβ CDR3 regions were amplified, and 750 ng of extracted DNA was sequenced by Adaptive Biotechnologies Corp. using the "deep" resolution ImmunoSEQ assay, as previously described (*53*). Raw sequence data were filtered using the Adaptive Biotechnologies website on the basis of the TCRβ V(D)J gene definitions provided by the International ImMunoGeneTics (IMGT) collaboration (*54*) using the IMGT database (www.imgt.org). Productive nucleotide sequences were used for all tracking experiments. The data were further filtered to exclude sequences with no identifiable V and J, removing PCR errors such as primer dimer and mispriming, as well as sequences with a raw read count <2, removing nucleotide sequencing errors (*29*).

### CTL tracking by HTTCS

Only cells that bound pMHC multimers were selected by flow cytometry before DNA isolation for HTTCS. The limit of detection of HTTCS was set to 0.001% for all TCR reads below which frequency could not be reliably determined (*31*). Only clonotypes present in the CTL products were tracked in PBMCs obtained after infusions. The frequency of each clonotype detected by HTTCS is based on all TCR Vβ reads from $CD4^+$ and $CD8^+$ T cells.

### Normal donor sorts

PBMCs were collected from three healthy adult donors and processed into three populations for TCR sequencing, that is, whole PBMCs, flow-sorted $CD3^+CD45RA^+$, and $CD3^+CD45RO^+$, representing the naïve and antigen-experienced T cell populations, respectively. TCRs from ~1 million cells from each population were sequenced by HTTCS. Clonotypes were tracked in the original PBMC samples and considered part of a $CD3^+CD45RA^+$ phenotype versus a $CD3^+CD45RO^+$ phenotype if it was observed in one population but not the other or if its abundance was 10-fold greater in one population than the other.

### Statistical analysis

Correlation between values was obtained by HTTCS, multimer, and TCR PCR: the Pearson's $R$ was calculated on the log TCR frequency using frequencies obtained by HTTCS and either percent $multimer^+$ T cells or TCR copies per 100 cells and treating each biological sample (i.e., time point) as an independent observation. $P$ values were generated by normal approximation. Half-lives of persistent TCR clonotypes were determined using the formula $t_{1/2} = t/(\log_2[N_0/Nt])$. Only clonotypes that had at least three consecutive values above the limit of detection (0.001%) and for which $R^2$ was >0.3 were used in the analysis. Comparison of clonotype $t_{1/2}$ was obtained in patients grouped according to their best clinical response: the Wilcoxon rank sum test was used to obtain $P$ values.

## SUPPLEMENTARY MATERIALS

immunology.sciencemag.org/cgi/content/full/2/8/eaal2568/DC1

Fig. S1. Naïve versus antigen-experienced phenotype based on clonotype frequency in PBMCs.

Table S1. Total, productive, and unique sequences in each sample.

Table S2. Identical results obtained by standard PCR and HTTCS for infused monoclonal products.

Table S3. Clonotype composition of monoclonal and polyclonal CTL products.

Table S4. Clinical responses of patients with metastatic melanoma who received polyclonal CTL products.

Table S5. Ki67 expression of transferred $multimer^+$ CTLs in patients who achieved CRs.

## REFERENCES AND NOTES


1. L. Gattinoni, C. A. Klebanoff, N. P. Restifo, Paths to stemness: Building the ultimate antitumour T cell. *Nat. Rev. Cancer* **12**, 671–684 (2012).
2. I. M. Stromnes, T. M. Schmitt, A. G. Chapuis, S. R. Hingorani, P. D. Greenberg, Re-adapting T cells for cancer therapy: From mouse models to clinical trials. *Immunol. Rev.* **257**, 145–164 (2014).
3. C. Yee, J. A. Thompson, D. Byrd, S. R. Riddell, P. Roche, E. Celis, P. D. Greenberg, Adoptive T cell therapy using antigen-specific $CD8^+$ T cell clones for the treatment of patients with metastatic melanoma: In vivo persistence, migration, and antitumor effect of transferred T cells. *Proc. Natl. Acad. Sci. U.S.A.* **99**, 16168–16173 (2002).
4. W. Y. Ho, H. N. Nguyen, M. Wolfl, J. Kuball, P. D. Greenberg, In vitro methods for generating $CD8^+$ T-cell clones for immunotherapy from the naive repertoire. *J. Immunol. Methods* **310**, 40–52 (2006).
5. N. N. Hunder, H. Wallen, J. Cao, D. W. Hendricks, J. Z. Reilly, R. Rodmyre, A. Jungbluth, S. Gnjatic, J. A. Thompson, C. Yee, Treatment of metastatic melanoma with autologous CD4+ T cells against NY-ESO-1. *N. Engl. J. Med.* **358**, 2698–2703 (2008).
6. H. Wallen, J. A. Thompson, J. Zachary Reilly, R. M. Rodmyre, J. Cao, C. Yee, Fludarabine modulates immune response and extends in vivo survival of adoptively transferred CD8 T cells in patients with metastatic melanoma. *PLOS ONE* **4**, e4749 (2009).
7. A. G. Chapuis, J. A. Thompson, K. A. Margolin, R. Rodmyre, I. P. Lai, K. Dowdy, E. A. Farrar, S. Bhatia, D. E. Sabath, J. Cao, Y. Li, C. Yee, Transferred melanoma-specific $CD8^+$ T cells persist, mediate tumor regression, and acquire central memory phenotype. *Proc. Natl. Acad. Sci. U.S.A.* **109**, 4592–4597 (2012).
8. A. G. Chapuis, G. B. Ragnarsson, H. N. Nguyen, C. N. Chaney, J. S. Pufnock, T. M. Schmitt, N. Duerkopp, I. M. Roberts, G. L. Pogosov, W. Y. Ho, S. Ochsenreither, M. Wölfl, M. Bar, J. P. Radich, C. Yee, P. D. Greenberg, Transferred WT1-reactive $CD8^+$ T cells can mediate antileukemic activity and persist in post-transplant patients. *Sci. Transl. Med.* **5**, 174ra127 (2013).
9. L. Gattinoni, C. A. Klebanoff, D. C. Palmer, C. Wrzesinski, K. Kerstann, Z. Yu, S. E. Finkelstein, M. R. Theoret, S. A. Rosenberg, N. P. Restifo, Acquisition of full effector function in vitro paradoxically impairs the in vivo antitumor efficacy of adoptively transferred $CD8^+$ T cells. *J. Clin. Invest.* **115**, 1616–1626 (2005).
10. C. A. Klebanoff, L. Gattinoni, P. Torabi-Parizi, K. Kerstann, A. R. Cardones, S. E. Finkelstein, D. C. Palmer, P. A. Antony, S. T. Hwang, S. A. Rosenberg, T. A. Waldmann, N. P. Restifo, Central memory self/tumor-reactive $CD8^+$ T cells confer superior antitumor immunity compared with effector memory T cells. *Proc. Natl. Acad. Sci. U.S.A.* **102**, 9571–9576 (2005).
11. C. A. Klebanoff, L. Gattinoni, N. P. Restifo, Sorting through subsets: Which T-cell populations mediate highly effective adoptive immunotherapy? *J. Immunother.* **35**, 651–660 (2012).
12. S. M. Pollack, R. L. Jones, E. A. Farrar, I. P. Lai, S. M. Lee, J. Cao, V. G. Pillarisetty, B. L. Hoch, A. Gullett, M. Bleakley, E. U. Conrad, J. F. Eary, K. C. Shibuya, E. H. Warren, J. N. Carstens, S. Heimfeld, S. R. Riddell, C. Yee, Tetramer guided, cell sorter assisted production of clinical grade autologous NY-ESO-1 specific $CD8^+$ T cells. *J. Immunother. Cancer* **2**, 36 (2014).
13. R. Zeng, R. Spolski, S. E. Finkelstein, S. K. Oh, P. E. Kovanen, C. S. Hinrichs, C. A. Pise-Masison, M. F. Radonovich, J. N. Brady, N. P. Restifo, J. A. Berzofsky, W. J. Leonard, Synergy of IL-21 and IL-15 in regulating $CD8^+$ T cell expansion and function. *J. Exp. Med.* **201**, 139–148 (2005).
14. C. S. Hinrichs, R. Spolski, C. M. Paulos, L. Gattinoni, K. W. Kerstann, D. C. Palmer, C. A. Klebanoff, S. A. Rosenberg, W. J. Leonard, N. P. Restifo, IL-2 and IL-21 confer opposing differentiation programs to $CD8^+$ T cells for adoptive immunotherapy. *Blood* **111**, 5326–5333 (2008).
15. Y. Li, M. Bleakley, C. Yee, IL-21 influences the frequency, phenotype, and affinity of the antigen-specific CD8 T cell response. *J. Immunol.* **175**, 2261–2269 (2005).
16. Y. Li, C. Yee, IL-21–mediated Foxp3 suppression leads to enhanced generation of antigen-specific $CD8^+$ cytotoxic T lymphocytes. *Blood* **111**, 229–235 (2008).
17. C. S. Hinrichs, Z. A. Borman, L. Gattinoni, Z. Yu, W. R. Burns, J. Huang, C. A. Klebanoff, L. A. Johnson, S. P. Kerkar, S. Yang, P. Muranski, D. C. Palmer, C. D. Scott, R. A. Morgan, P. F. Robbins, S. A. Rosenberg, N. P. Restifo, Human effector $CD8^+$ T cells derived from naive rather than memory subsets possess superior traits for adoptive immunotherapy. *Blood* **117**, 808–814 (2011).
18. M. Wölfl, P. D. Greenberg, Antigen-specific activation and cytokine-facilitated expansion of naive, human $CD8^+$ T cells. *Nat. Protoc.* **9**, 950–966 (2014).
19. A. G. Chapuis, S. M. Lee, J. A. Thompson, I. M. Roberts, K. A. Margolin, S. Bhatia, H. L. Sloan, I. Lai, F. Wagener, K. Shibuya, J. Cao, J. D. Wolchok, P. D. Greenberg, C. Yee, Combined IL-21–primed polyclonal CTL plus CTLA4 blockade controls refractory metastatic melanoma in a patient. *J. Exp. Med.* **213**, 1133–1139 (2016).
20. A. G. Chapuis, I. M. Roberts, S. M. Lee, H. L. Sloan, I. P. Lai, E. A. Farrar, F. Wagener, K. C. Shibuya, J. Cao, P. D. Greenberg, C. Yee, T-cell therapy using interleukin-21–primed

cytotoxic T-cell lymphocytes combined with cytotoxic T-cell lymphocyte antigen-4 blockade results in long-term cell persistence and durable tumor regression. *J. Clin. Oncol.* **34**, 3787–3795 (2016).
21. E. J. Wherry, V. Teichgräber, T. C. Becker, D. Masopust, S. M. Kaech, R. Antia, U. H. von Andrian, R. Ahmed, Lineage relationship and protective immunity of memory CD8 T cell subsets. *Nat. Immunol.* **4**, 225–234 (2003).
22. C. Berger, M. C. Jensen, P. M. Lansdorp, M. Gough, C. Elliott, Adoptive transfer of effector $CD8^+$ T cells derived from central memory cells establishes persistent T cell memory in primates. *J. Clin. Invest.* **118**, 294–305 (2008).
23. E. E. West, B. Youngblood, W. G. Tan, H.-T. Jin, K. Araki, G. Alexe, B. T. Konieczny, S. Calpe, G. J. Freeman, C. Terhorst, W. N. Haining, R. Ahmed, Tight regulation of memory $CD8^+$ T cells limits their effectiveness during sustained high viral load. *Immunity* **35**, 285–298 (2011).
24. A. J. Mc Adam, A. N. Schweitzer, A. H. Sharpe, The role of B7 co-stimulation in activation and differentiation of $CD4^+$ and $CD8^+$ T cells. *Immunol. Rev.* **165**, 231–247 (1998).
25. M. Y. Kimura, L. A. Pobezinsky, T. I. Guinter, J. Thomas, A. Adams, J.-H. Park, X. Tai, A. Singer, IL-7 signaling must be intermittent, not continuous, during $CD8^+$ T cell homeostasis to promote cell survival instead of cell death. *Nat. Immunol.* **14**, 143–151 (2013).
26. F. Sallusto, D. Lenig, R. Forster, M. Lipp, A. Lanzavecchia, Two subsets of memory T lymphocytes with distinct homing potentials and effector functions. *Nature* **401**, 708–712 (1999).
27. S. C. De Rosa, L. A. Herzenberg, L. A. Herzenberg, M. Roederer, 11-color, 13-parameter flow cytometry: Identification of human naive T cells by phenotype, function, and T-cell receptor diversity. *Nat. Med.* **7**, 245–248 (2001).
28. S. M. Kaech, E. J. Wherry, R. Ahmed, Effector and memory T-cell differentiation: Implications for vaccine development. *Nat. Rev. Immunol.* **2**, 251–262 (2002).
29. H. S. Robins, P. V. Campregher, S. K. Srivastava, A. Wacher, C. J. Turtle, O. Kahsai, S. R. Riddell, E. H. Warren, C. S. Carlson, Comprehensive assessment of T-cell receptor β-chain diversity in αβ T cells. *Blood* **114**, 4099–4107 (2009).
30. H. S. Robins, S. K. Srivastava, P. V. Campregher, C. J. Turtle, J. Andriesen, S. R. Riddell, C. S. Carlson, E. H. Warren, Overlap and effective size of the human $CD8^+$ T cell receptor repertoire. *Sci. Transl. Med.* **2**, 47ra64 (2010).
31. H. Robins, C. Desmarais, J. Matthis, R. Livingston, J. Andriesen, H. Reijonen, C. Carlson, G. Nepom, C. Yee, K. Cerosaletti, Ultra-sensitive detection of rare T cell clones. *J. Immunol. Methods* **375**, 14–19 (2012).
32. A. G. Chapuis, O. K. Afanasiev, J. G. Iyer, K. G. Paulson, U. Parvathaneni, J. Ha Hwang, I. Lai, I. M. Roberts, H. L. Sloan, S. Bhatia, K. C. Shibuya, T. Gooley, C. Desmarais, D. M. Koelle, C. Yee, P. Nghiem, Regression of metastatic Merkel cell carcinoma following transfer of polyomavirus-specific T cells and therapies capable of re-inducing HLA class-I. *Cancer Immunol. Res.* **2**, 27–36 (2014).
33. J. D. Wolchok, A. Hoos, S. O'Day, J. S. Weber, O. Hamid, C. Lebbé, M. Maio, M. Binder, O. Bohnsack, G. Nichol, R. Humphrey, F. Stephen Hodi, Guidelines for the evaluation of immune therapy activity in solid tumors: Immune-related response criteria. *Clin. Cancer Res.* **15**, 7412–7420 (2009).
34. C. M. Bollard, S. Gottschalk, A. M. Leen, H. Weiss, K. C. Straathof, G. Carrum, M. Khalil, M.-. Wu, M. Helen Huls, C.-C. Chang, M. Victoria Gresik, A. P. Gee, M. K. Brenner, C. M. Rooney, H. E. Heslop, Complete responses of relapsed lymphoma following genetic modification of tumor-antigen presenting cells and T-lymphocyte transfer. *Blood* **110**, 2838–2845 (2007).
35. R. A. Morgan, M. E. Dudley, J. R. Wunderlich, M. S. Hughes, J. C. Yang, R. M. Sherry, R. E. Royal, S. L. Topalian, U. S. Kammula, N. P. Restifo, Z. Zheng, A. Nahvi, C. R. de Vries, L. J. Rogers-Freezer, S. A. Mavroukakis, S. A. Rosenberg, Cancer regression in patients after transfer of genetically engineered lymphocytes. *Science* **314**, 126–129 (2006).
36. E. J. Wherry, M. Kurachi, Molecular and cellular insights into T cell exhaustion. *Nat. Rev. Immunol.* **15**, 486–499 (2015).
37. G. Makedonas, N. Hutnick, D. Haney, A. C. Amick, J. Gardner, G. Cosma, A. R. Hersperger, D. Dolfi, E. J. Wherry, G. Ferrari, M. R. Betts, Perforin and IL-2 upregulation define qualitative differences among highly functional virus-specific human $CD8^+$ T cells. *PLOS Pathog.* **6**, e1000798 (2010).
38. L. Gattinoni, E. Lugli, Y. Ji, Z. Pos, C. M. Paulos, M. F. Quigley, J. R. Almeida, E. Gostick, Z. Yu, C. Carpenito, E. Wang, D. C. Douek, D. A. Price, C. H. June, F. M. Marincola, M. Roederer, N. P. Restifo, A human memory T cell subset with stem cell–like properties. *Nat. Med.* **17**, 1290–1297 (2011).
39. E. Lugli, M. H. Dominguez, L. Gattinoni, P. K. Chattopadhyay, D. L. Bolton, K. Song, N. R. Klatt, J. M. Brenchley, M. Vaccari, E. Gostick, D. A. Price, T. A. Waldmann, N. P. Restifo, G. Franchini, M. Roederer, Superior T memory stem cell persistence supports long-lived T cell memory. *J. Clin. Invest.* **123**, 594–599 (2013).
40. G. Oliveira, E. Ruggiero, M. Teresa Lupo Stanghellini, N. Cieri, M. D'Agostino, R. Fronza, C. Lulay, F. Dionisio, S. Mastaglio, R. Greco, J. Peccatori, A. Aiuti, A. Ambrosi, L. Biasco, A. Bondanza, A. Lambiase, C. Traversari, L. Vago, C. von Kalle, M. Schmidt, C. Bordignon, F. Ciceri, C. Bonini, Tracking genetically engineered lymphocytes long-term reveals the dynamics of T cell immunological memory. *Sci. Transl. Med.* **7**, 317ra198 (2015).
41. E. Lugli, L. Gattinoni, A. Roberto, D. Mavilio, D. A. Price, N. P. Restifo, M. Roederer, Identification, isolation and in vitro expansion of human and nonhuman primate T stem cell memory cells. *Nat. Protoc.* **8**, 33–42 (2013).
42. W. Cui, Y. Liu, J. S. Weinstein, J. Craft, S. M. Kaech, An interleukin-21-interleukin-10-STAT3 pathway is critical for functional maturation of memory $CD8^+$ T cells. *Immunity* **35**, 792–805 (2011).
43. Y. Tian, M. A. Cox, S. M. Kahan, J. T. Ingram, R. K. Bakshi, A. J. Zajac, A context-dependent role for IL-21 in modulating the differentiation, distribution, and abundance of effector and memory CD8 T cell subsets. *J. Immunol.* **196**, 2153–2166 (2016).
44. L. C. Osborne, N. Abraham, Regulation of memory T cells by γc cytokines. *Cytokine* **50**, 105–113 (2010).
45. J. N. Blattman, R. Antia, D. J. D. Sourdive, X. Wang, S. M. Kaech, K. Murali-Krishna, J. D. Altman, R. Ahmed, Estimating the precursor frequency of naive antigen-specific CD8 T cells. *J. Exp. Med.* **195**, 657–664 (2002).
46. V. I. Zarnitsyna, B. D. Evavold, L. N. Schoettle, J. N. Blattman, R. Antia, Estimating the diversity, completeness, and cross-reactivity of the T cell repertoire. *Front. Immunol.* **4**, 485 (2013).
47. P. C. Tumeh, C. L. Harview, J. H. Yearley, I. P. Shintaku, E. J. M. Taylor, L. Robert, B. Chmielowski, M. Spasic, G. Henry, V. Ciobanu, A. N. West, M. Carmona, C. Kivork, E. Seja, G. Cherry, A. J. Gutierrez, T. R. Grogan, C. Mateus, G. Tomasic, J. A. Glaspy, R. O. Emerson, H. Robins, R. H. Pierce, D. A. Elashoff, C. Robert, A. Ribas, PD-1 blockade induces responses by inhibiting adaptive immune resistance. *Nature* **515**, 568–571 (2014).
48. J. D. Stone, D. M. Kranz, Role of T cell receptor affinity in the efficacy and specificity of adoptive T cell therapies. *Front. Immunol.* **4**, 244 (2013).
49. J. D. Stone, D. T. Harris, D. M. Kranz, TCR affinity for p/MHC formed by tumor antigens that are self-proteins: Impact on efficacy and toxicity. *Curr. Opin. Immunol.* **33**, 16–22 (2015).
50. F. Garrido, N. Aptsiauri, E. M. Doorduijn, A. M. Garcia Lora, T. van Hall, The urgent need to recover MHC class I in cancers for effective immunotherapy. *Curr. Opin. Immunol.* **39**, 44–51 (2016).
51. M. Hebeisen, M. Allard, P. O. Gannon, J. Schmidt, D. E. Speiser, N. Rufer, Identifying individual T cell receptors of optimal avidity for tumor antigens. *Front. Immunol.* **6**, 582 (2015).
52. F. S. Hodi, S. J. O'Day, D. F. McDermott, R. W. Weber, J. A. Sosman, J. B. Haanen, R. Gonzalez, C. Robert, D. Schadendorf, J. C. Hassel, W. Akerley, A. J. M. van den Eertwegh, J. Lutzky, P. Lorigan, J. M. Vaubel, G. P. Linette, D. Hogg, C. H. Ottensmeier, C. Lebbé, C. Peschel, I. Quirt, J. I. Clark, J. D. Wolchok, J. S. Weber, J. Tian, M. J. Yellin, G. M. Nichol, A. Hoos, W. J. Urba, Improved survival with ipilimumab in patients with metastatic melanoma. *N. Engl. J. Med.* **363**, 711–723 (2010).
53. A. M. Sherwood, Deep sequencing of the human TCRγ and TCRβ repertoires suggests that TCRβ rearranges after αβ and γδ T cell commitment. *Sci. Transl. Med.* **3**, 90ra61 (2011).
54. M. Yousfi Monod, V. Giudicelli, D. Chaume, M. P. Lefranc, IMGT/JunctionAnalysis: The first tool for the analysis of the immunoglobulin and T cell receptor complex V-J and V-D-J JUNCTIONs. *Bioinformatics* **20** (suppl. 1), i379–i385 (2004).

**Acknowledgments:** The described work was performed at the FHCRC. **Funding:** This work was supported by the Cancer Research Institute and by the Stand Up To Cancer, Cancer Immunology Dream Team Translational Research Grant (SU2C-AACR-DT1012). Stand Up To Cancer is a program of the Entertainment Industry Foundation administered by the American Association for Cancer Research (AACR). A.G.C. was supported by the NIH Laboratory–oriented K08 Career Development Award and the Damon Runyon Fellowship Award. C.Y. was supported by the Burroughs Wellcome Fund Translational Scientist Award and is co-leader of the Stand Up To Cancer–AACR/Cancer Research Institute Immunology Dream Team. **Author contributions:** A.G.C. designed the experiments, analyzed and interpreted the data, and drafted the manuscript. C.D. supervised the HTTCS data generation and analyzed and interpreted the data. K.C.S., I.P.L., F.W., and I.M.R. generated the CTL products and performed the experiments including DNA isolation, tracking using multimer, and PCR assays. J.C., D.G.C., T.M.S., P.D.G., E.H.W., and H.R. participated in research conception and design and analyzed and interpreted the data. R.E. performed the statistics and normal donor studies. C.Y. supervised the research, analyzed and interpreted the data, and revised the manuscript. All authors edited and approved the manuscript. **Competing interests:** The authors declare that they have no competing interests. C.Y. is a member of the Parker Institute for Cancer Immunotherapy and on the advisory board of Adaptive Biotechnologies, whose technology was used to sequence the TCRs. A conflict management board was established at the FHCRC when these assays were performed.

Submitted 25 October 2016
Accepted 12 January 2017
Published 24 February 2017
10.1126/sciimmunol.aal2568

**Citation:** A. G. Chapuis, C. Desmarais, R. Emerson, T. M. Schmitt, K. C. Shibuya, I. P. Lai, F. Wagener, J. Chou, I. M. Roberts, D. G. Coffey, E. H. Warren, H. Robins, P. D. Greenberg, C. Yee, Tracking the fate and origin of clinically relevant adoptively transferred $CD8^+$ T cells in vivo. *Sci. Immunol.* **2**, eaal2568 (2017).

Science Immunology

# Tracking the fate and origin of clinically relevant adoptively transferred CD8+ T cells in vivo

Aude G. Chapuis, Cindy Desmarais, Ryan Emerson, Thomas M. Schmitt, Kendall C. Shibuya, Ivy P. Lai, Felecia Wagener, Jeffrey Chou, Ilana M. Roberts, David G. Coffey, Edus H. Warren, Harlan Robins, Philip D. Greenberg, and Cassian Yee

*Sci. Immunol.*, **2** (8), eaal2568.
DOI: 10.1126/sciimmunol.aal2568

**Tracking tumor immunity**
Tumor-specific immune cells can lead to tumor regression in some cancer patients who do not respond to other therapies; however, the ability to track these cells after transfer has remained limited. Now, Chapuis *et al.* use high-throughput T cell receptor V# sequencing (HTTCS) to track individual clonotypes after transfer. They find that very low frequency clonotypes with proliferative and survival advantages can contribute to long-term tumor control. These data will help guide the selection of cell populations for immunotherapy.